COMPDYN 2011
III ECCOMAS Thematic Conference on
Computational Methods in Structural Dynamics and Earthquake Engineering
M. Papadrakakis, M. Fragiadakis, V. Plevris (eds.)
Corfu, Greece, 25–28 May 2011

SEISMIC DESIGN METHODOLOGY FOR CONTROL OF 3D BUILDINGS BY MEANS OF MULTIPLE TUNED-MASS-DAMPERS

Yael Daniel[1] **and Oren Lavan**[2]

[1] Faculty of Civil and Environmental Engineering, Technion – Israel Institute of Technology
Technion City, Haifa 32000, Israel
e-mail: yaeldan@tx.technion.ac.il

[2] Faculty of Civil and Environmental Engineering, Technion – Israel Institute of Technology
Technion City, Haifa 32000, Israel
e-mail: lavan@tx.technion.ac.il

Keywords: Seismic Control, Tuned-Mass-Dampers, Dynamic Vibration Absorbers, Fully-Stressed Design, Multiple Mode Vibration.

Abstract. *This paper presents a methodology for the optimal design of multiple Tuned Mass Dampers (TMDs) in 3D irregular buildings. The objective function minimizes the total mass of all added TMDs. Constraints are added to limit the total accelerations experienced at the edges of the floors in the direction parallel to each edge. The formulation of the design methodology relies on optimality criteria conjectured herein, hence, a two stage iterative analysis/redesign procedure that is based on analysis tools only is resulted. This allows the application of the methodology in a practical design process.*

1 INTRODUCTION

Seismic protection of structures is an important issue in structural design due to its threatening consequences. Often, it is required that the design of a structure provide even more than life safety, promising a certain level of serviceability following a severe earthquake, while allowing for a defined level of damage, i.e. performance-based design. Damage to structural components is often linked to inter-story drifts, when considering damage due to maximal responses, and to energy dissipation when considering damage due to cumulative actions. When considering damage to acceleration sensitive non-structural elements, total accelerations (which are accelerations in respect to an inertial frame of reference, also referred to as absolute accelerations) produced during the ground-motion are of most interest. Total acceleration levels are also very important when considering the comfort level of human occupancy. In addition, total accelerations have an effect on base-shear and overturning moments [1].

There is ample literature on the control of these responses through control devices that reduce the energy dissipation demand of the structure. Several passive damping devices are available, including viscous and visco-elastic dampers, and metallic and friction hysteretic dampers [1, 2]. Another device to be used herein is the Tuned-Mass-Damper (TMD). Details about TMDs and their applications may be found in the fine works [1, 3, 4, 5, 6], only to name a few.

The use of TMDs for the reduction of responses of tall buildings due to wind loadings became widespread [7, 8, 9]. With efficient seismic design strategies, those devices may be attractive for multi-hazard mitigation of both winds and earthquakes. While wind-induced vibrations are usually dominated by a single mode, using TMDs for seismic structural protection is more complicated. In seismic vibrations, no single distinct frequency dominates the behavior, but rather many frequencies, including the ones of higher modes. Many researchers are therefore hesitant in using TMDs for seismic structural applications [10, 11, 12, 13, 14]. It should be noted that most of those works use only a single TMD tuned to a fundamental frequency. In addition, a TMD relies on tuning the device's natural frequency as to suppress the vibration of the structure, based on the structure's natural frequencies. However, if detuning occurs, the device loses much of its efficiency.

One solution to these drawbacks may be found in active or semi-active TMDs (ATMDs or SATMDs), whose frequencies may be altered at each moment [15, 16, 17, 18]. Active control, however, requires an external power source to be activated, which may be costly and may force a reliability issue during an actual earthquake. Another possible solution may be achieved using multiple TMDs (MTMDs), each tuned to a different frequency. This may lead to a solution that controls various frequencies for various modes of the structure. Those TMDs could also be distributed along the structure and located at locations which will optimize the control of the structure. In addition, each TMD that is aimed at controlling a certain mode of the structure could be split to several TMDs, each tuned to a slightly different frequency within a bandwidth close to the natural frequency of the main system, thus reducing the detuning effect and allowing design robustness (for example [19]). The idea of using MTMDs tuned to various natural frequencies of the structure and distributed along its height is not new. Clark [20] indicated that a single TMD can not significantly reduce the motion created due to seismic excitations, while MTMDs can substantially reduce motion. Moon [21, 22] shows a practical application of vertically-distributed MTMDs in tall buildings for reducing wind-induced vibrations, and offers a method of distributing them by mode shape. In his work, dampers are located at the perimeter in the space between the inner and outer façade layers in double skin façade systems, as their vibrations are in the direction perpendicular to the edge of the floor. In the methodology presented herein a somewhat different approach is

taken, as the dampers' vibrations are in parallel to the floor edge. This allows a better control of torsional response as well as larger strokes for the dampers.

Several methodologies for the optimal design of a single passive TMD for MDOF structures exist, each using a different objective function [8, 23, 24, 25]. Hadi and Arfiadi [26] use an H_2 performance index to retrieve the optimal parameter of a TMD added to a MDOF structure. H_2 and H_∞ optimization criteria are also widely used in ATMD problems (for example [27]). The H_2 approach minimizes a weighted average of the weighted sum of responses at various locations, and the control energy input. In the case of passive control, however, the control energy input is not a relevant cost measure. The H_∞ approach, on the other hand, minimizes the worst case energy attenuation of the controlled output with respect to an excitation of a given energy. Here, however, the characteristics of the input motion expected at the site where the structure is located are not considered. It should be emphasized that both approaches make use of smeared measures of the controlled responses rather than limiting each local response separately. In buildings in general, however, (see for example [28, 29]), and in the case of irregular buildings in particular, it is highly important to limit each local response separately. In addition, both approaches do not target an allowable response limit. In the context of the last two highly important issues, Bounded State Control (BSC) seems more appropriate since local states are each bounded to allowable limits [28, 29].

Bounded State Control algorithms can be roughly categorized into two groups. The first relies on a train of high energy pulses of control forces (e.g. [29, 30] and references therein) while the second makes use of a continuous control law (e.g. [31, 32, 33). While may be attractive in the application of an active control system, the pulse control strategies are not likely to be implemented by passive means. The methods that make use of continuous control laws, on the other hand, usually require formal optimization.

There are not many methodologies available for the design of MTMDs of various frequencies and locations in seismic application. In their pioneering work, Chen and Wu [34] use a frequency based transfer function as a response measure of the multi-modal vibration problem of structures. Rather than solving a formal optimization problem, they use a sequential search technique in order to allocate multi-modal MTMDs. A pre-assumed number of TMDs is sequentially added at locations where the location index (which, for example, can be the location of maximal root-mean-square (RMS) acceleration prior to placement of each damper) is optimal in each sequence. Luo et al. [35] also dealt with the multi-modal vibration problem of structures using MTMDs. In their work, a dynamic magnification factor (DMF) of the first mode obtained based on the transfer function of the structure's response in frequency domain is minimized. Constraints on the DMFs of other modes are also considered. Lin et al. [36] proposed a two-stage frequency-domain based optimal design of MTMDs taking into consideration both the structural response and the TMD stroke, and found that there is a good balance between limiting the TMD stroke and not substantially compromising on structural response. Fu and Johnson [37] suggest using passive MTMDs with a vertical distribution of mass, where each story is assigned with one TMD of which its' parameters (mass, stiffness and inherent damping) are optimized as to minimize the sum of inter-story drifts. The optimization problem is solved using a pattern-search, and a local minimum is obtained. While the above methodologies present a huge step forward, there is still no methodology that leads to a desired performance under a realistic representation of the ground motion hazard, in small computational efforts while using analysis tools only.

This paper presents a simple frequency-domain performance-based methodology for solving the allocation and sizing problem of multi-modal MTMDs in structures undergoing seismic excitations. The objective function minimizes the total mass of all added TMDs. Constraints are added to limit the total accelerations experienced at the edges of the floors in

the direction parallel to each edge. The methodology is based on a simple iterative analysis/redesign procedure where first, an analysis is performed for a given design and then redesign of the TMDs is performed according to recurrence relations. The redesign first determines the mass of all dampers at a given location based on RMS acceleration (peak acceleration could be indirectly used). Then this mass is distributed between dampers tuned to various frequencies. The methodology is based on the simple optimal design parameters of TMDs presented by Den-Hartog [3] and Warburton [4] to successfully reduce the acceleration demands within the structure. The advantages of the proposed methodology is its simplicity, relaying on analyses tools only, it is performance-based - catered to serve any desirable performance, and its fast convergence.

2 PROBLEM FORMULATION

2.1 Equations of motion

Following Soong [29], the equations of motion of a MDOF system can be represented in state-space notation as:

$$\begin{aligned}\dot{\hat{\mathbf{x}}}(t) &= \mathbf{A}\cdot\hat{\mathbf{x}}(t)+\mathbf{B}\cdot a_g(t)\\ \mathbf{y}(t) &= \mathbf{CC}\cdot\hat{\mathbf{x}}(t)\end{aligned} \tag{1}$$

where $\hat{\mathbf{x}}^{\mathrm{T}}=\left[\mathbf{x}^{\mathrm{T}}\quad \dot{\mathbf{x}}^{\mathrm{T}}\right]$; $\mathbf{x}\in R^N$, $\hat{\mathbf{x}}\in R^{2N}$ is the state variable vector, $\mathbf{x}(t)$ is the displacement vector between the DOFs and the ground, $a_g(t)$ is the ground-motion's acceleration, a dot represents the derivative with respect to time, and $\mathbf{y}(t)$ is the output vector of the system, whose entries are responses of interest. Those responses are a linear combination of the state variables and the input forces (in our case $\mathbf{y}(t)=\mathbf{x}(t)$). The matrices **A**, **B** and **CC** are defined as following:

$$\mathbf{A}=\begin{bmatrix}\mathbf{0}_{N\times N} & \mathbf{I}_{N\times N}\\ -\mathbf{M}^{-1}\mathbf{K} & -\mathbf{M}^{-1}\mathbf{C}\end{bmatrix}\quad \mathbf{B}=\begin{bmatrix}\mathbf{0}_{N\times 1}\\ -\mathbf{e}\end{bmatrix}\quad \mathbf{CC}=\begin{bmatrix}\mathbf{I}_{N\times N} & \mathbf{0}_{N\times N}\end{bmatrix} \tag{2}$$

where **M**, **C** and **K** are the mass, inherent damping and stiffness matrices of the structure according to the chosen *N* degrees-of-freedom (DOFs), respectively, **e** is the excitation direction vector with values of zero and one, **I** is the identity matrix and **0** is a zero matrix of appropriate dimensions, as noted.

It should be noted that for the sake of presentation, Eq. (1) and the following methodology are presented using a single input (component of the ground motion). An extension to the case of multiple inputs simultaneously, or multiple components of the ground motion in different directions, is straightforward.

2.2 Performance measures

Sensitivity of equipment within the structure, as well as human discomfort is found to be most dependent on total accelerations produced within the structure during an earthquake [1, 34]. The acceleration serviceability limit of structures is thus a suitable performance criterion for design. Reducing the drift levels within the structure is also a goal that should be reckoned with, as drifts are the main source of structural damage. This criterion is not directly taken into consideration in the present work; however, as will be seen in the example, using the proposed methodology leads to a considerable reduction of peak drifts as well. Moreover, some structures are expected to lead to acceptable, or close to acceptable, drifts even without

retrofitting, but to be sensitive to total accelerations. One example for that is buildings for which wind loads dictate the design for lateral loads. Here, earthquakes may still lead to high total accelerations. Hence, total accelerations serve in this paper as the performance measure of the structure.

Added TMDs help control the responses of the structure, and the measure of cost of this controlling system is by the amount of added mass. As more mass is added to the structure, the retrofit is said to be more expensive and thus less cost-effective.

2.3 Problem formulation

The problem at hand is formulated as an optimization problem for which the objective function minimizes the total amount of added masses in the TMDs under constraints of maximal performance measures. The total accelerations at all peripheral locations of all floors are taken as the performance measures, as they are the largest accelerations expected within story limits. Those locations are shown in Fig. 1 as: $(\mathbf{x}_{\text{pyl}})_n$, $(\mathbf{x}_{\text{pyr}})_n$, $(\mathbf{x}_{\text{pxt}})_n$ and $(\mathbf{x}_{\text{pxb}})_n$, and are the peripheral coordinates in the "y", "y", "x" and "x" directions, at the left, right, top and bottom edges of floor n, respectively. The remaining variables will be explained subsequently. That is, the constraints are on the total accelerations at the edges of all floors in the directions parallel to each edge. The optimization problem is thus formulated as:

$$\begin{aligned} &\min J = \sum_{l}^{\substack{\text{all}\\ \text{locations}}} \sum_{f}^{\substack{\text{all}\\ \text{frequencies}}} \left(\mathbf{m}_{\text{TMD}}\right)_{l,f} \\ &s.t. \\ &\frac{\max\limits_{eq}\left(\max\limits_{t}\left(\left(\ddot{\mathbf{x}}_{\text{p}}^{\text{t}}(t)\right)_l\right)\right)}{a_{\text{all}}^{\text{t}}} \le 1.0 \qquad \forall l = 1,2,...,N_{locations} \end{aligned} \tag{3}$$

where $(\mathbf{m}_{\text{TMD}})_{l,f}$ is the mass of the TMD located at peripheral location l tuned to frequency f, $\max\limits_{eq}\left(\max\limits_{t}\left(\left(\ddot{\mathbf{x}}_{\text{p}}^{\text{t}}(t)\right)_l\right)\right)$ is the envelope of peak total acceleration in time at each location, l, under all considered earthquakes, $a_{\text{all}}^{\text{t}}$ is the allowable total acceleration, and $N_{locations}$ is the number of locations to be constrained (=$4N_{floors}$ where N_{floors} is the number of floors). The peripheral locations, l, are ordered such that the vector of peripheral coordinates is $\mathbf{x}_{\text{p}}=[\mathbf{x}_{\text{pyl}}^{\text{T}}\ \mathbf{x}_{\text{pyr}}^{\text{T}}\ \mathbf{x}_{\text{pxt}}^{\text{T}}\ \mathbf{x}_{\text{pxb}}^{\text{T}}]^{\text{T}}$ (see also Fig. 1). It should be noted that with a slight modification, the methodology to follow could also constrain the total accelerations of the floors' corners in any direction, if desired.

Rather than directly solving the time-domain representation of the problem (Eq. (3)), the proposed methodology uses an equivalent frequency-domain representation, introducing peripheral RMS total accelerations rather than peripheral peak total accelerations. The allowed values for the RMS total accelerations are properly scaled so as to lead to the desired allowable peak accelerations in time of Eq. (3). In frequency-domain, Eq. (3) is transformed into:

$$\begin{aligned} &\min J = \sum_{l}^{\substack{\text{all}\\ \text{locations}}} \sum_{f}^{\substack{\text{all}\\ \text{frequencies}}} \left(\mathbf{m}_{TMD}\right)_{l,f} \\ &s.t. \\ &\frac{RMS\left(\left(\ddot{\mathbf{x}}_{\text{p}}^{\text{t}}\right)_l\right)}{a_{\text{all}}^{\text{RMS}}} \le 1.0 \qquad \forall l = 1,2,...,N_{locations} \end{aligned} \tag{4}$$

where $a_{\text{all}}^{\text{RMS}}$ is the allowable RMS total acceleration and $RMS\left(\left(\ddot{\mathbf{x}}_{\text{p}}^{\text{t}}\right)_l\right)$ is the root mean square of the total acceleration at location l (the l^{th} term of $RMS\left(\ddot{\mathbf{x}}_{\text{p}}^{\text{t}}\right)$). Such reference to a component of a vector or a matrix, i.e. $(\cdot)_l$, will be used throughout the paper.

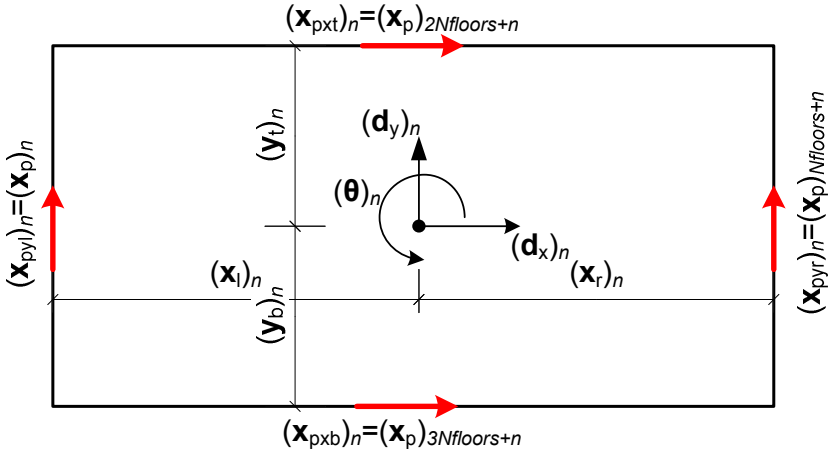

Figure 1: Definition of dynamic DOFs and peripheral coordinates of the n$^{\text{th}}$ floor.

3 PROPOSED SOLUTION SCHEME

3.1 Fully-stressed design (FSD)

Designs that are based on fully stressed characteristics go back to the classical design of trusses under static loads, whereby the weight is minimized for a given allowable stress. For that problem, it had been widely accepted that the optimal design yields a: statically determinate fully stressed design, with members out of the design having strains smaller than the allowable. This result appeared in the literature as early as 1900 as: “A statically determined framework of included figure is the most economic form of a framework of given indeterminate figure for the support of a given loading” [38]. It was later shown that this design is a Karush-Kuhn-Tucker point and therefore, an optimal design [39].

Recently, it was shown that some dynamic optimal designs also possess "fully stressed" characteristics. Levy and Lavan [40] considered the minimization of total added viscous damping to frame structures subjected to ground accelerations, while constraining various inter-story responses. Their optimal solutions attained by formal optimization indicated that: "At the optimum, damping is assigned to stories for which the local performance index has reached the allowable value. Stories with no assigned damping attain a local performance index which is lower or equal to the allowable." That is, the optimal solutions attained "fully stressed" characteristics.

Based on past experience of the authors in similar problems, it is conjectured here that the optimal solution to MTMD allocation and sizing in structures (the solution of Eq. (4)) possesses FSD characteristics, i.e.:

At the optimum, TMDs are assigned to peripheral locations for which the RMS total acceleration has reached the allowable value under the considered input acceleration PSD. In addition, at each location to which TMDs are added, TMDs of a given frequency are assigned only to frequencies for which the output spectral density is maximal.

Potential locations for TMDs are located at the edges of the floors, as their lines of action are in direction parallel to the edges (Fig. 2). Those are actually the same locations where total accelerations are to be limited. The coordinates "**z**" in Fig. 2 will be explained subsequently.

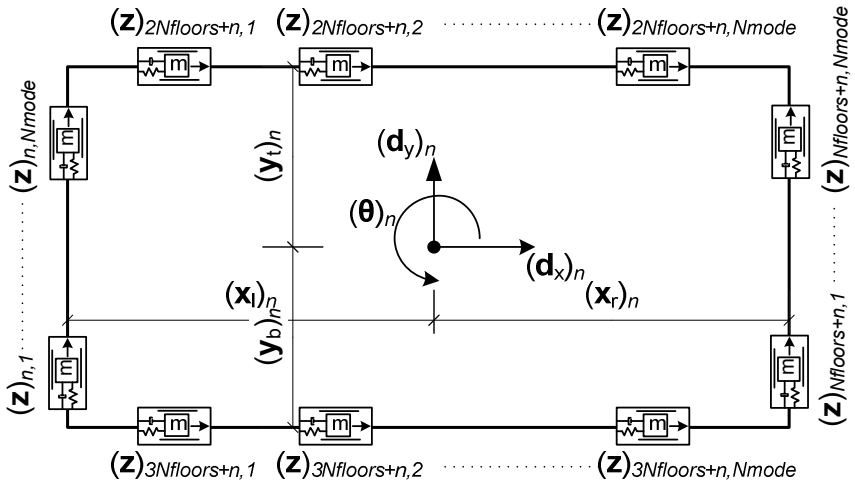

Figure 2: Locations of TMDs at the floor n and their associated z DOFs.

Stage one of the conjecture, imposes that for all peripheral locations with masses within the design, the total acceleration equals the allowable one, while all peripheral locations with zero masses (outside the design) have an acceleration equal to or less than the allowable. This is illustrated on the left-hand side of Fig. 3, which presents the concept on a selected peripheral frame. Here, the 5th floor is the only on to be dampened ($\sum_f \left(\mathbf{m}_{\mathrm{TMD}}\right)_{5,f} \neq 0$), as it is the only floor to reach the allowable RMS acceleration. The second stage of the conjecture imposes that for all dampers at a peripheral location where the acceleration equals the allowable one, and are within the design, the output spectral densities are maximal (with respect to ω) and equal. As for masses outside of the design at this DOF, the output spectral density is less than maximal. This is illustrated on the right-hand side of Fig. 3 where $\left(\mathbf{R}_{\ddot{\mathbf{x}}_{\mathrm{p}}^{\mathrm{t}}}(\omega)\right)_l$ is the output spectral density for the total acceleration at the location l (=5 in Fig. 3). As can be seen, $\left(\mathbf{m}_{\mathrm{TMD}}\right)_{5,1}$ and $\left(\mathbf{m}_{\mathrm{TMD}}\right)_{5,2}$ are the only ones with a mass larger than zero as their output spectral densities, $\left(\mathbf{R}_{\ddot{\mathbf{x}}_{\mathrm{p}}^{\mathrm{t}}}(\omega)\right)_5$, are largest. It should be noted that if the desired constraints are on the corners' total accelerations in any direction, dampers would be added to the direction that contributes more to the acceleration (between x and y).

The above conjecture suggests that the tuning frequency of each TMD is searched for amongst all possible frequencies. However, for practical reasons, it is reasonable to assume that these frequencies are in the vicinity of the bare structure's frequencies, and thus the tuning of TMDs could be in relation to the bare structure's natural frequency.

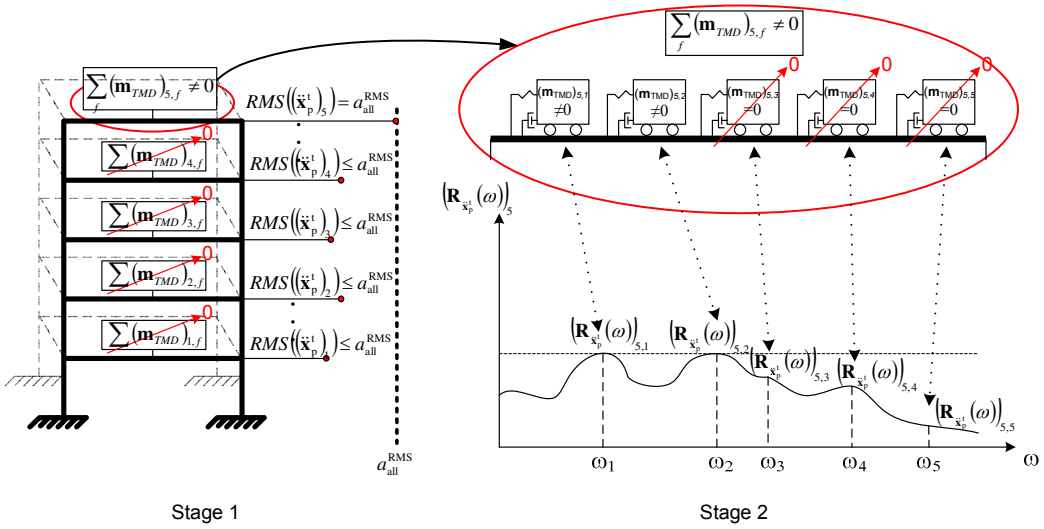

Figure 3: Illustrations of the first part of the conjecture (left) and the second part of the conjecture (right).

3.2 Analysis/Redesign algorithm

Solutions to optimization problems, which possess fully stressed characteristics, are efficiently achieved iteratively using a two step algorithm in each iteration cycle. In the first step, an analysis is performed for a given preliminary design, whereas in the second step the design is changed using a recurrence relationship that targets fully stressedness. The recurrence relation can be generally written as:

$$x_l^{(n+1)} = x_l^{(n)} \cdot \left(\frac{pi_l^{(n)}}{pi_{allowable}} \right)^P \tag{5}$$

where x_l is the value of the design variable associated with the location l, pi_l is the performance measure of interest for the location l, $pi_{allowable}$ is the allowable value for the performance measure, n - the iteration number and P - a convergence parameter. Fully stressedness is obtained from using Eq. (5) since upon convergence one of the following must take place. Either $x_l^{(n+1)} = x_l^{(n)}$ giving $pi_l^{(n)} = pi_{allowable}$, or $x_l^{(n+1)} = x_l^{(n)} = 0$ giving $pi_l^{(n)} \le pi_{allowable}$.

In the optimal design of trusses, for example, the engineer would assume initial values for the cross sections as design variables (x_l's in Eq. (5)) and run an analysis. Then, based on the attained stresses as the performance measures (pi_l's in Eq. (5)), and their allowable values, the cross section of each bar could be redesigned using Eq. (5). The process could be repeated until convergence. The advantages of the analysis/redesign algorithm include its simplicity, the need to use analysis tools only, and the fairly small computational effort that lies in the small number of analyses required for convergence. Such analysis/redesign procedure will be utilized here to attain fully stressed designs where the mass, frequency and locations of MTMDs within framed structures is to be determined.

4 DESIGN METHODOLOGY

The proposed design methodology relies on the analysis/redesign procedure which leads to the FSD criteria presented above. The proposed methodology is summarized in the following flowchart. Following the flowchart is an extensive elaboration of each step, including the equations referred to within the flowchart.

4.1 Stepwise flowchart

Initial actions

1. Determine the mass, stiffness and inherent damping matrices of the structure. Decide on allowable RMS accelerations, which should represent the desired peak total acceleration.
2. Determine the natural frequencies and mode shapes of the structure.
3. Decide on an input PSD, which should represent an ensemble of chosen ground-motions (see example). For each DOF, evaluate the total acceleration transfer function in frequency domain using Eq. (8), transform this transfer function into peripheral coordinates using Eq. (10) and determine the peripheral output spectral density using Eq. (11). The peripheral RMS acceleration is derived from Eq. (12).
4. Add N_{mode} (N_{mode} being the number of modes potentially damped) TMDs at each peripheral coordinate, each tuned to one frequency of the structure, with the initial properties described in Eqs. (14), (17) and (19).

Iterative action

5. Update the mass, stiffness and damping matrices of the structure with the added damping system, using Eqs. (20) - (25).
6. Re-evaluate the RMS accelerations excited within the structure using Eqs. (8) - (12). Notice that for Eq. (8) the expressions $\mathbf{M}^{-1}\mathbf{K}$ and $\mathbf{M}^{-1}\mathbf{C}$ are taken from Eqs. (26) and (27), to avoid singularity.
7. Redesign the mass of each TMD according to the recurrence formulas given in Eqs. (28) and (29). Accordingly, reevaluate the stiffness and damping coefficient of each TMD using Eqs. (15) - (19).
8. Repeat steps 5 to 7 until convergence of the mass is reached.
9. Validate the results using time-history analysis and the selected set of ground-motions.
10. If desired, the allowable RMS acceleration may be scaled according to the reduction of envelope peak acceleration determined in step 9 and the allowable peak acceleration in time domain, using Eq. (30), followed by repeating steps 5-9 until fully satisfied.

Step 1: A desired maximal RMS acceleration (representing the desired peak total acceleration) is chosen. The mass, damping and stiffness matrices of the structure are assembled according to the relevant dynamic DOFs, which in the case of the simplest n^{th} floor of a 3D structure are two perpendicular displacements of a chosen coordinate and the floor's rotation, as noted in Fig. 1 by "$(\mathbf{d}_x)_n$", "$(\mathbf{d}_y)_n$" and "$(\boldsymbol{\theta})_n$". As it is desired to control peripheral responses (which include the largest responses within floor limits in the "x" and "y" directions), a coordinate transformation from floor DOFs to peripheral coordinates is performed as follows:

$$\mathbf{x}_p = \mathbf{T} \cdot \mathbf{x} \tag{6}$$

where $\mathbf{x}=\left[\mathbf{d}_x^{\mathrm{T}} \quad \mathbf{d}_y^{\mathrm{T}} \quad \boldsymbol{\theta}^{\mathbf{T}}\right]^{\mathbf{T}}$ and the transformation matrix $\mathbf{T}$ is:

$$\underset{(4\cdot N_{floors}x3\cdot N_{floors})}{\mathbf{T}}=\begin{bmatrix} \underset{(N_{floors}xN_{floors})}{\mathbf{0}} & \underset{(N_{floors}xN_{floors})}{\mathbf{I}} & \underset{(N_{floors}xN_{floors})}{diag(\mathbf{x_l})} \\ \underset{(N_{floors}xN_{floors})}{\mathbf{0}} & \underset{(N_{floors}xN_{floors})}{\mathbf{I}} & \underset{(N_{floors}xN_{floors})}{diag(\mathbf{x_r})} \\ \underset{(N_{floors}xN_{floors})}{\mathbf{I}} & \underset{(N_{floors}xN_{floors})}{\mathbf{0}} & \underset{(N_{floors}xN_{floors})}{-diag(\mathbf{y_t})} \\ \underset{(N_{floors}xN_{floors})}{\mathbf{I}} & \underset{(N_{floors}xN_{floors})}{\mathbf{0}} & \underset{(N_{floors}xN_{floors})}{-diag(\mathbf{y_b})} \end{bmatrix} \tag{7}$$

where N_{floors} is the number of floors, N is the number of DOFs and $\mathbf{x_l}$, $\mathbf{x_r}$, $\mathbf{y_t}$, and $\mathbf{y_b}$ are the distances from the DOFs' coordinate system's origin to the left, right, top and bottom edges, ordered from first to top floor, as shown for the story n in Fig. 1.

Step 2: Solution of the eigenvalue problem determines the structure's natural frequencies and mode shapes.

Step 3: A power spectral density (PSD) for the input acceleration is chosen. Examples of such input spectrums are stationary white-noise, which gives a constant PSD, and the Kanai-Tajimi PSD [41]. Additional PSDs for ground-motional modeling can be found in Nagarajaiah and Narasimhan [42] and in Agrawal et al. [43]. The PSD is fitted to represent real ground-motions. This is done by fitting its parameters to a frequency-based spectrum, representing the decomposition of earthquakes into frequency components (for example, a FFT spectrum). For each DOF, the transfer function of total acceleration of the bare frame is evaluated using Eq. (8). This transfer function represents the ratio between the sinusoidal output amplitude to a sinusoidal input amplitude with frequency ω.

For total accelerations it can be shown that the appropriate transfer vector, $\mathbf{H}_{\ddot{\mathbf{x}}^{\mathrm{t}}}(j\omega)$, is:

$$\mathbf{H}_{\ddot{\mathbf{x}}^{\mathrm{t}}}(j\omega)=-\mathbf{M}^{-1}\cdot(j\omega\mathbf{C}+\mathbf{K})\cdot\mathbf{H}_{\mathbf{x}}(j\omega) \tag{8}$$

where $j=\sqrt{-1}$ and $\mathbf{H}_{\mathbf{x}}(j\omega)$ is the displacement transfer vector [44], given by:

$$\mathbf{H}_{\mathbf{x}}(j\omega)=\mathbf{CC}\cdot(j\omega\mathbf{I}-\mathbf{A})^{-1}\cdot\mathbf{B} \tag{9}$$

This transfer function is transformed to peripheral coordinates using:

$$\mathbf{H}_{\ddot{\mathbf{x}}_{\mathrm{p}}^{\mathrm{t}}}(j\omega)=\mathbf{T}\cdot\mathbf{H}_{\ddot{\mathbf{x}}^{\mathrm{t}}}(j\omega) \tag{10}$$

where $\mathbf{H}_{\ddot{\mathbf{x}}_{\mathrm{p}}^{\mathrm{t}}}(j\omega)$ is the structure's transfer function of total accelerations in peripheral coordinates. The output spectral densities of the peripheral accelerations, $\left(\mathbf{R}_{\ddot{\mathbf{x}}_{\mathrm{p}}^{\mathrm{t}}}(\omega)\right)_l$, are evaluated using:

$$\left(\mathbf{R}_{\ddot{\mathbf{x}}_{\mathrm{p}}^{\mathrm{t}}}(\omega)\right)_l=\left|\left(\mathbf{H}_{\ddot{\mathbf{x}}_{\mathrm{p}}^{\mathrm{t}}}(j\omega)\right)_l\right|^2\cdot S(\omega) \tag{11}$$

where $S(\omega)$is the input PSD, $\left|\left(\mathbf{H}_{\ddot{\mathbf{x}}_{\mathrm{p}}^{\mathrm{t}}}(j\omega)\right)_l\right|^2=\left(\mathbf{H}_{\ddot{\mathbf{x}}_{\mathrm{p}}^{\mathrm{t}}}(j\omega)\right)_l\cdot\left(\mathbf{H}^{*}_{\ddot{\mathbf{x}}_{\mathrm{p}}^{\mathrm{t}}}(j\omega)\right)_l$ where $\left(\mathbf{H}_{\ddot{\mathbf{x}}^{\mathrm{t}}}(j\omega)\right)_l$ is the l^{th} term of $\mathbf{H}_{\ddot{\mathbf{x}}^{\mathrm{t}}}(j\omega)$, $\left(\mathbf{H}^{*}_{\ddot{\mathbf{x}}^{\mathrm{t}}}(j\omega)\right)_l$ is its complex conjugate.

The area under the output spectral density curve equals the mean-square response [45], and thus, the root-mean-square (RMS) of total accelerations at peripheral coordinate l, $RMS\left(\ddot{\mathbf{x}}_{\mathrm{p}}^{\mathrm{t}}\right)_l$,taking into consideration the contribution of all frequencies to the total response, is derived using:

$$RMS\left(\ddot{\mathbf{x}}_{\mathrm{p}}^{\mathrm{t}}\right)_l = \sqrt{2\cdot\int_0^{\infty}\left(\mathbf{R}_{\ddot{\mathbf{x}}_{\mathrm{p}}^{\mathrm{t}}}(\omega)\right)_l d\omega} \tag{12}$$

Step 4: If for any peripheral coordinate, l, the RMS acceleration obtained is larger than the allowable RMS acceleration, MTMDs are added to suppress the acceleration produced. Each TMD of mass $(\mathbf{m}_{\mathrm{TMD}})_{l,f}$ is assigned with a DOF for its displacement relative to the ground, $(\mathbf{z})_{l,f}$. Here, the subscript l stands for its location while the subscript f stands for its frequency. The location, l, is corresponding to the peripheral coordinate $(\mathbf{x}_{\mathrm{p}})_l$ the TMD is attached to. At each location, N_{mode} TMDs are added, to suppress N_{mode} original frequencies of the structure, where N_{mode} is the number of modes to potentially be controlled. Thus, generally a total of $N_{mode}\cdot N_{locations}$ dampers are potentially added (Fig. 2). Note that the order of DOFs in the damped structure is:

$$\tilde{\mathbf{x}} = \left[\mathbf{d}_x^{\mathrm{T}} \quad \mathbf{d}_y^{\mathrm{T}} \quad \boldsymbol{\theta}^{\mathrm{T}} \quad (\mathbf{z})_{1,1} \quad (\mathbf{z})_{2,1} \quad \cdots \quad (\mathbf{z})_{N_{locations},1} \quad \cdots \quad (\mathbf{z})_{1,N_{mode}} \quad (\mathbf{z})_{2,N_{mode}} \quad \cdots \quad (\mathbf{z})_{N_{locations},N_{mode}}\right]^{\mathrm{T}} \tag{13}$$

Note the difference between the coordinates $(\mathbf{x}_{\mathrm{p}})_l$ to the coordinates $(\mathbf{z})_{l,f}$. While the coordinates $(\mathbf{x}_{\mathrm{p}})_l$ relate to peripheral displacements of the floors themselves, $(\mathbf{z})_{l,f}$ relate to displacements of the masses of TMDs relative to the ground. Note also that those two vectors are organized such that the component l of $\mathbf{z}$ relates to the displacement of a TMD that is attached to the floor at the location of the component l of $\mathbf{x}_{\mathrm{p}}$, i.e. the locations l are corresponding in those two vectors.

The initial properties of each such damper are obtained based on a SDOF system representing the damped mode. In this work, Den-Hartog's properties [3] were chosen. These properties were derived for the optimal reduction of mass displacement of a SDOF system under external sinusoidal loading. They were later shown to also reduce the maximum total acceleration response of the mass of a SDOF system undergoing a harmonic base excitation [4]. It should be noted that any different set of chosen properties (mass, stiffness and inherent damping of each TMD) can be easily used with the proposed scheme instead of Den-Hartog. In the case of optimal Den-Hartog properties:

1. For each peripheral coordinate, the initial mass of all TMDs located at that coordinate is taken as certain predetermined percentage of the structure's mass (say 1%). It is divided equally between the dampers situated at the same location:

$$\left(\mathbf{m}_{\mathrm{TMD}}\right)_{l,f} = \frac{0.01}{N_{mode}}\cdot M_{structure} \tag{14}$$

where l represents the damper's location, f represents the mode dampened and $M_{structure}$ is the structure's total mass. The mass ratio $\left(\boldsymbol{\mu}_{\mathrm{TMD}}\right)_f$ of all TMDs tuned to frequency f equals the ratio between the effective TMD mass of all TMDs tuned to frequency f and the f^{th} modal mass of the structure. This mass ratio is defined as:

$$\left(\boldsymbol{\mu}_{\mathrm{TMD}}\right)_f = \frac{\boldsymbol{\phi}_f^{\mathrm{T}}\cdot\mathbf{T}^{\mathrm{T}}\cdot\mathcal{D}\left(\left(\mathbf{m}_{\mathrm{TMD}}\right)_f\right)\cdot\mathbf{T}\cdot\boldsymbol{\phi}_f}{\boldsymbol{\phi}_f^{\mathrm{T}}\cdot\mathbf{M}_{\mathbf{original}}\cdot\boldsymbol{\phi}_f} \tag{15}$$

where ϕ_f is the f^{th} mode-shape of the bare structure, $\left[\mathbf{M_{original}}\right]$ is the bare frame's mass matrix, $\mathbf{T}$ is the transformation matrix of Eq. (7), and $\mathcal{D}\left(\left(\mathbf{m}_{\mathrm{TMD}}\right)_f\right)$ is a diagonal matrix with the terms $\left(\mathbf{m}_{\mathrm{TMD}}\right)_{1:Nlocations,f}$ sitting on the diagonal in the order of TMD DOFs, as in Eq. (13).

2. Each TMD's stiffness is determined according to the frequency of the mode which is dampened by the TMD. The frequency is tuned to:

$$\left(\boldsymbol{\omega}_{\mathrm{TMD}}\right)_f = \frac{\left(\boldsymbol{\omega}_{\mathrm{n}}\right)_f}{1+\left(\boldsymbol{\mu}_{\mathrm{TMD}}\right)_f} \tag{16}$$

where $\left(\boldsymbol{\omega}_{\mathrm{n}}\right)_f$ is the frequency f to be dampened. The compatible stiffness is:

$$\left(\mathbf{k}_{\mathrm{TMD}}\right)_{l,f} = \left(\mathbf{m}_{\mathrm{TMD}}\right)_{l,f} \cdot \left(\left(\boldsymbol{\omega}_{\mathrm{TMD}}\right)_f\right)^2 \tag{17}$$

3. Each TMD's modal damping ratio is determined according to:

$$\left(\boldsymbol{\xi}_{\mathrm{TMD}}\right)_f = \sqrt{\frac{3\cdot\left(\boldsymbol{\mu}_{\mathrm{TMD}}\right)_f}{8\cdot\left(1+\left(\boldsymbol{\mu}_{\mathrm{TMD}}\right)_f\right)^3}} \tag{18}$$

and the matching damping coefficient:

$$\left(\mathbf{c}_{\mathrm{TMD}}\right)_{l,f} = 2\cdot\left(\mathbf{m}_{\mathrm{TMD}}\right)_{l,f} \cdot \left(\boldsymbol{\xi}_{\mathrm{TMD}}\right)_f \cdot \left(\boldsymbol{\omega}_{\mathrm{n}}\right)_f \tag{19}$$

Step 5: The mass, damping and stiffness matrices of the damped frame are formulated, using the following. The new mass matrix is:

$$\mathbf{M} = \begin{bmatrix} \left[\mathbf{M_{original}} + \mathbf{B_{dm}}^{\mathrm{T}}\mathbf{m_{TMD}}\mathbf{B_{dm}}\right] & \mathbf{0} \\ \mathbf{0} & \left[\mathbf{m_{TMD}}\right] \end{bmatrix} \tag{20}$$

where $\left[\mathbf{M_{original}}\right]$ is the bare frame's mass matrix and $\left[\mathbf{m_{TMD}}\right]$ is a diagonal matrix with the terms $\left(\mathbf{m}_{\mathrm{TMD}}\right)_{l,f}$ sitting on the diagonal in the order of TMD DOFs, as in Eq. (13). The matrix $\mathbf{B_{dm}}$ is a transfer matrix, used to add the mass of TMDs to the mass of the structure perpendicular to their original DOF (i.e. if a certain damper is used to reduce vibration in the "y" direction, and thus its DOF is in the "y" direction, the mass of that TMD is added to the mass of the structure in the "x" direction of the story where it is situated). It is given by:

$$\mathbf{B_{dm}}^{\mathrm{T}} = \begin{bmatrix} 1 & . & . & . & . & . & N_m \\ \mathbf{T_m}^{\mathrm{T}} & . & . & . & . & . & \mathbf{T}_{\mathbf{a_m}}^{\mathrm{T}} \end{bmatrix} \tag{21}$$

where:

$$\underset{(4\cdot N_{floors}x3\cdot N_{floors})}{\mathbf{T_m}} = \begin{bmatrix} \underset{(N_{floors}xN_{floors})}{\mathbf{I}} & \underset{(N_{floors}xN_{floors})}{\mathbf{0}} & \underset{(N_{floors}xN_{floors})}{\mathbf{0}} \\ \underset{(N_{floors}xN_{floors})}{\mathbf{I}} & \underset{(N_{floors}xN_{floors})}{\mathbf{0}} & \underset{(N_{floors}xN_{floors})}{\mathbf{0}} \\ \underset{(N_{floors}xN_{floors})}{\mathbf{0}} & \underset{(N_{floors}xN_{floors})}{\mathbf{I}} & \underset{(N_{floors}xN_{floors})}{\mathbf{0}} \\ \underset{(N_{floors}xN_{floors})}{\mathbf{0}} & \underset{(N_{floors}xN_{floors})}{\mathbf{I}} & \underset{(N_{floors}xN_{floors})}{\mathbf{0}} \end{bmatrix} \tag{22}$$

The damping matrix of the damped frame is constructed as:

$$\mathbf{C} = \begin{bmatrix} \left[\mathbf{C}_{\mathbf{original}} + \mathbf{B_d}^{\mathrm{T}}\mathbf{c}_{\mathbf{TMD}}\mathbf{B_d}\right] & \left[-\mathbf{B_d}^{\mathrm{T}}\mathbf{c}_{\mathbf{TMD}}\right] \\ \left[-\mathbf{c}_{\mathbf{TMD}}\mathbf{B_d}\right] & \left[\mathbf{c}_{\mathbf{TMD}}\right] \end{bmatrix} \tag{23}$$

where $\left[\mathbf{C}_{\mathbf{original}}\right]$ is the bare frame's inherent damping matrix and $\left[\mathbf{c}_{\mathbf{TMD}}\right]$ is a diagonal matrix with the terms $\left(\mathbf{c}_{\mathrm{TMD}}\right)_{l,f}$ sitting on the diagonal in the order of DOFs as in Eq. (13). The matrix $\mathbf{B_d}$ is a transfer matrix, used to assign the TMDs within the structure.

$$\mathbf{B_d}^{\mathrm{T}} = \begin{matrix} 1 & . & . & . & . & . & N_m \\ \end{matrix} \\ \begin{bmatrix} \mathbf{T}^{\mathrm{T}} & . & . & . & . & . & \overset{o}{\mathbf{T}}^{\mathrm{T}} \end{bmatrix} \tag{24}$$

The stiffness matrix of the damped frame is constructed similarly as:

$$\mathbf{K} = \begin{bmatrix} \left[\mathbf{K}_{\mathbf{original}} + \mathbf{B_d}^{\mathrm{T}}\mathbf{k}_{\mathbf{TMD}}\mathbf{B_d}\right] & \left[-\mathbf{B_d}^{\mathrm{T}}\mathbf{k}_{\mathbf{TMD}}\right] \\ \left[-\mathbf{k}_{\mathbf{TMD}}\mathbf{B_d}\right] & \left[\mathbf{k}_{\mathbf{TMD}}\right] \end{bmatrix} \tag{25}$$

where $\left[\mathbf{K}_{\mathbf{original}}\right]$ is the bare frame's stiffness matrix and $\left[\mathbf{k}_{\mathbf{TMD}}\right]$ is a diagonal matrix with the terms $\left(\mathbf{k}_{\mathrm{TMD}}\right)_{l,f}$ sitting on the diagonal in the order of DOFs as in Eq. (13).

Step 6: The peripheral RMS accelerations of the damped frame at all coordinates are evaluated using frequency-domain analysis based on Eqs. (8) - (12), using the newly-updated matrices (note that in Eq. (12) it is needed to take only the first *N* components of the extended vector $\mathbf{H}_{\ddot{\tilde{\mathbf{x}}}}(j\omega)$ as now DOFs of TMDs are included in this vector). As earlier mentioned, this requires the evaluation of each DOF's transfer function. As the computation of the transfer function involves inversion of the mass matrix, and some TMD masses may get very small during the design process, singularity issues may occur. To avoid those, the expressions $\mathbf{M^{-1}K}$ and $\mathbf{M^{-1}C}$ used in Eq. (2) are evaluated as follows:

$$\mathbf{M^{-1}K} = \begin{bmatrix} \left(\mathbf{M}_{\mathbf{original}} + \mathbf{B_{dm}}^{\mathrm{T}}\mathbf{m}_{\mathbf{TMD}}\mathbf{B_{dm}}\right)^{-1} \cdot \left(\mathbf{K}_{\mathbf{original}} + \mathbf{B_d}^{\mathrm{T}}\mathbf{k}_{\mathbf{TMD}}\mathbf{B_d}\right) & -\left(\mathbf{M}_{\mathbf{original}} + \mathbf{B_{dm}}^{\mathrm{T}}\mathbf{m}_{\mathbf{TMD}}\mathbf{B_{dm}}\right)^{-1}\mathbf{B_d}^{\mathrm{T}}\mathbf{k}_{\mathbf{TMD}} \\ -\mathbf{\Omega}^2_{\mathbf{TMD}}\mathbf{B_d} & \mathbf{\Omega}^2_{\mathbf{TMD}} \end{bmatrix} \tag{26}$$

where $\mathbf{\Omega}^2_{\mathbf{TMD}}$ is a diagonal matrix with the terms $\left(\left(\boldsymbol{\omega}_{\mathrm{TMD}}\right)_{l,f}\right)^2$ sitting on the diagonal in the order of DOFs given in Eq. (13), and:

$$\mathbf{M^{-1}C} = \begin{bmatrix} \left(\mathbf{M}_{\mathbf{original}} + \mathbf{B_{dm}}^{\mathrm{T}}\mathbf{m}_{\mathbf{TMD}}\mathbf{B_{dm}}\right)^{-1} \cdot \left(\mathbf{C}_{\mathbf{original}} + \mathbf{B_d}^{\mathrm{T}}\mathbf{c}_{\mathbf{TMD}}\mathbf{B_d}\right) & -\left(\mathbf{M}_{\mathbf{original}} + \mathbf{B_{dm}}^{\mathrm{T}}\mathbf{m}_{\mathbf{TMD}}\mathbf{B_{dm}}\right)^{-1}\mathbf{B_d}^{\mathrm{T}}\mathbf{c}_{\mathbf{TMD}} \\ -\mathbf{\Omega\xi}_{\mathbf{TMD}}\mathbf{B_d} & \mathbf{\Omega\xi}_{\mathbf{TMD}} \end{bmatrix} \tag{27}$$

where $\mathbf{\Omega\xi}_{\mathbf{TMD}}$ is a diagonal matrix with the terms $2\cdot\left(\boldsymbol{\xi}_{\mathrm{TMD}}\right)_{l,f}\cdot\left(\boldsymbol{\omega}_{\mathrm{TMD}}\right)_{l,f}$ sitting on the diagonal in the order of DOFs given in Eq. (13).

Step 7: The TMD's mass is re-determined using two stages; the total mass of all dampers located at a given location is determined, followed by the distribution of that mass between all

TMDs at that location, having various tuning frequencies. This is done according to the recurrence relationships described below. Following the change in mass, the stiffness and modal damping ratio of each TMD are also updated while keeping the Den-Hartog principles intact, using Eqs. (15) - (19). The two-stage analysis/redesign procedure is carried out iteratively, in the following way.

Stage 1: The first stage of redesign includes the evaluation of the total mass of all TMDs at a certain location, which promises the existence of the first part of the conjecture. This is formulated using:

$$\left(\mathbf{m}_{\text{TMD,total}}^{(n+1)}\right)_l = \sum_{f=1}^{\substack{\text{all}\\ \text{frequencies}}} \left(\mathbf{m}_{\text{TMD}}^{(n+1)}\right)_{l,f} = \sum_{f=1}^{\substack{\text{all}\\ \text{frequencies}}} \left(\mathbf{m}_{\text{TMD}}^{(n)}\right)_{l,f} \cdot \left(\frac{RMS\left(\left(\ddot{\mathbf{x}}_{\text{p}}^{\text{t}\,(n)}\right)_l\right)}{a_{\text{all}}^{\text{RMS}}} \right)^P \tag{28}$$

where $(\cdot)^{(n)}$ is the value at iteration n, $\left(\mathbf{m}_{\text{TMD,total}}^{(n+1)}\right)_l$ is the total mass of all dampers at location l, and P is a constant which influences the convergence and convergence rate. A large P will result in a faster but less stable convergence of the above equation. Based on the authors' experience, a P in the range of 0.1-2.0 should be satisfying in terms of stability, convergence and fair amount of iterations.

Stage 2: In the second stage of redesign, the total mass obtained at each location is distributed between N_{mode} dampers (dampening modes $\left(\boldsymbol{\omega}_{\text{n}}\right)_f$) at that same location l, promising the existence of the second part of the conjecture, using the following:

$$\left(\mathbf{m}_{\text{TMD}}^{(n+1)}\right)_{l,f} = \left(\mathbf{m}_{\text{TMD}}^{(n)}\right)_{l,f} \left(\frac{\sqrt{\left(\mathbf{R}_{\ddot{\mathbf{x}}_{\text{p}}^{\text{t}}}^{(n)}\left(\left(\boldsymbol{\omega}_{\text{n}}\right)_f\right)\right)_l}}{\max\limits_f\left(\sqrt{\left(\mathbf{R}_{\ddot{\mathbf{x}}_{\text{p}}^{\text{t}}}^{(n)}\left(\left(\boldsymbol{\omega}_{\text{n}}\right)_f\right)\right)_l}\right)} \right)^P \cdot \frac{\left(\mathbf{m}_{\text{TMD,total}}^{(n+1)}\right)_l}{\sum\limits_{f=1}^{\substack{\text{all}\\ \text{frequencies}}} \left(\mathbf{m}_{\text{TMD}}^{(n)}\right)_{l,f} \left(\frac{\sqrt{\left(\mathbf{R}_{\ddot{\mathbf{x}}_{\text{p}}^{\text{t}}}^{(n)}\left(\left(\boldsymbol{\omega}_{\text{n}}\right)_f\right)\right)_l}}{\max\limits_f\left(\sqrt{\left(\mathbf{R}_{\ddot{\mathbf{x}}_{\text{p}}^{\text{t}}}^{(n)}\left(\left(\boldsymbol{\omega}_{\text{n}}\right)_f\right)\right)_l}\right)} \right)^P} \tag{29}$$

where $\left(\mathbf{R}_{\ddot{\mathbf{x}}_{\text{p}}^{\text{t}}}^{(n)}\left(\left(\boldsymbol{\omega}_{\text{n}}\right)_f\right)\right)_l$ is the component of $\mathbf{R}_{\ddot{\mathbf{x}}_{\text{p}}^{\text{t}}}^{(n)}(\omega)$ at the location l evaluated at $\omega = \left(\boldsymbol{\omega}_{\text{n}}\right)_f$.

The analysis/redesign procedure is continued until convergence. It shall be noted that each iteration cycle may result in either a bigger or smaller mass.

Rational: Upon convergence, i.e when values at the iteration $n+1$ are equal to the corresponding values at the iteration n, Eq. (28) is satisfied under one of two conditions. That is, either $\sum_{f=1}^{\text{all frequencies}} \left(\mathbf{m}_{\text{TMD}}^{(n+1)}\right)_{l,f} = \sum_{f=1}^{\text{all frequencies}} \left(\mathbf{m}_{\text{TMD}}^{(n)}\right)_{l,f} \neq 0$ and thus $RMS\left(\left(\ddot{\mathbf{x}}_{\text{p}}^{\text{t}\,(n+1)}\right)_l\right) = RMS\left(\left(\ddot{\mathbf{x}}_{\text{p}}^{\text{t}\,(n)}\right)_l\right) = a_{\text{all}}^{\text{RMS}}$, or $RMS\left(\left(\ddot{\mathbf{x}}_{\text{p}}^{\text{t}\,(n+1)}\right)_l\right) = RMS\left(\left(\ddot{\mathbf{x}}_{\text{p}}^{\text{t}\,(n)}\right)_l\right) \leq a_{\text{all}}^{\text{RMS}}$ and then $\sum_{f=1}^{\text{all frequencies}} \left(\mathbf{m}_{\text{TMD}}^{(n+1)}\right)_{l,f} = \sum_{f=1}^{\text{all frequencies}} \left(\mathbf{m}_{\text{TMD}}^{(n)}\right)_{l,f} = 0$. This portrays fully-stressedness in total accelerations, i.e. the first part of the conjecture. Eq. (29), on the other hand, portrays fully-stressedness in frequency response. Here, taking the sum of each side of the equation with respect to f implies that the sum of masses of TMDs at the location l and iteration $n+1$ equals the desired total mass from the first stage, $\left(\mathbf{m}_{\text{TMD,total}}^{(n+1)}\right)_l$, or $\sum_{f=1}^{\text{all frequencies}} \left(\mathbf{m}_{\text{TMD}}^{(n+1)}\right)_{l,f} = \left(\mathbf{m}_{\text{TMD,total}}^{(n+1)}\right)_l$. This is actually attained using the fraction on the right-hand side

of Eq. (29), which is constant for all f's. The remaining part of Eq. (29) has a similar structure to that of Eq. (28). That is, upon convergence, either $\left(\mathbf{m}_{\mathrm{TMD}}^{(n+1)}\right)_{l,f}=\left(\mathbf{m}_{\mathrm{TMD}}^{(n)}\right)_{l,f}\neq 0$ and thus $\sqrt{\left(\mathbf{R}_{\ddot{\mathbf{x}}_{\mathrm{p}}^{\mathrm{t}}}^{(n)}\left(\left(\boldsymbol{\omega}_{\mathrm{n}}\right)_f\right)\right)_l}=\max_f\left(\sqrt{\left(\mathbf{R}_{\ddot{\mathbf{x}}_{\mathrm{p}}^{\mathrm{t}}}^{(n)}\left(\left(\boldsymbol{\omega}_{\mathrm{n}}\right)_f\right)\right)_l}\right)$, or $\sqrt{\left(\mathbf{R}_{\ddot{\mathbf{x}}_{\mathrm{p}}^{\mathrm{t}}}^{(n)}\left(\left(\boldsymbol{\omega}_{\mathrm{n}}\right)_f\right)\right)_l}\leq\max_f\left(\sqrt{\left(\mathbf{R}_{\ddot{\mathbf{x}}_{\mathrm{p}}^{\mathrm{t}}}^{(n)}\left(\left(\boldsymbol{\omega}_{\mathrm{n}}\right)_f\right)\right)_l}\right)$ and then $\left(\mathbf{m}_{\mathrm{TMD}}^{(n+1)}\right)_{l,f}=\left(\mathbf{m}_{\mathrm{TMD}}^{(n)}\right)_{l,f}=0$. This portrays fully-stressedness in frequency response, i.e. the second part of the conjecture. It should be noted that the normalization of $\sqrt{\left(\mathbf{R}_{\ddot{\mathbf{x}}_{\mathrm{p}}^{\mathrm{t}}}^{(n)}\left(\left(\boldsymbol{\omega}_{\mathrm{n}}\right)_f\right)\right)_l}$ with respect to $\max_f\left(\sqrt{\left(\mathbf{R}_{\ddot{\mathbf{x}}_{\mathrm{p}}^{\mathrm{t}}}^{(n)}\left(\left(\boldsymbol{\omega}_{\mathrm{n}}\right)_f\right)\right)_l}\right)$ has no effect on the results of this equation and is done here only for clarification of the rational behind Eq. (29).

Step 8: Repeat steps 5 to 7 until convergence of the mass is reached.

Step 9: After the process converges, the retrofitted frame's response is validated using time history analysis for all ground-motions within the chosen ensemble.

Step 10: The percent of reduction in RMS acceleration and the percent of reduction of envelope peak accelerations in time domain may not be entirely compatible. Thus, a modification of the allowable RMS acceleration may be performed as to scale these two frequency/time domain measures, using the following:

$$a_{\mathrm{all},l}^{\mathrm{RMS}}=a_{\mathrm{all}}^{\mathrm{t}}\cdot\frac{RMS\left(\left(\ddot{\mathbf{x}}_{\mathrm{p}}^{\mathrm{t}}\right)_l\right)}{\max_{eq}\left(\max_t\left(\left(\ddot{\mathbf{x}}_{\mathrm{p}}^{\mathrm{t}}(t)\right)_l\right)\right)}\qquad\forall l=1,2,.....,N_{locations}\tag{30}$$

where: $a_{\mathrm{all},l}^{\mathrm{RMS}}$ is the modified allowable RMS acceleration to be used in the frequency-domain analysis.

Once the allowable RMS acceleration is re-scaled, steps 5-9 are repeated until the reduction in peak acceleration is as desired in the performance-based design.

5 EXAMPLE

The following 8-story asymmetric RC frame structure (Fig. 4) introduced by Tso and Yao [46] is retrofitted using MTMDs for an excitation in the "y" direction. A uniform distributed mass of 0.75 ton/m^2 is taken. The column dimensions are 0.5m by 0.5m for frames 1 and 2 and 0.7m by 0.7m for frames 3 and 4. The beams are 0.4m wide and 0.6m tall. 5% Rayleigh damping for the first and second modes is used. A 40% reduction of the peripheral peak total acceleration obtained in the bare structure is desired. Hence, initially, an allowable peripheral RMS acceleration of 60% of the maximal peripheral RMS acceleration of the bare structure is adopted. The response is analyzed under a Kanai-Tajimi PSD with parameters fitted to the average FFT values of a chosen ensemble of ground-motions (SE 10 in 50). The design variables are the locations and properties of the individual tuned mass dampers. The dampers are to potentially be located in the peripheral frames, where they are most effective, and as the excitation is in the "y" direction only, dampers will be assigned only to peripheral frames 1 and 4, to dampen frequencies of modes which involve "y" and "θ". The ‘stepwise flowchart’ described above is closely followed to optimally design the MTMDs.

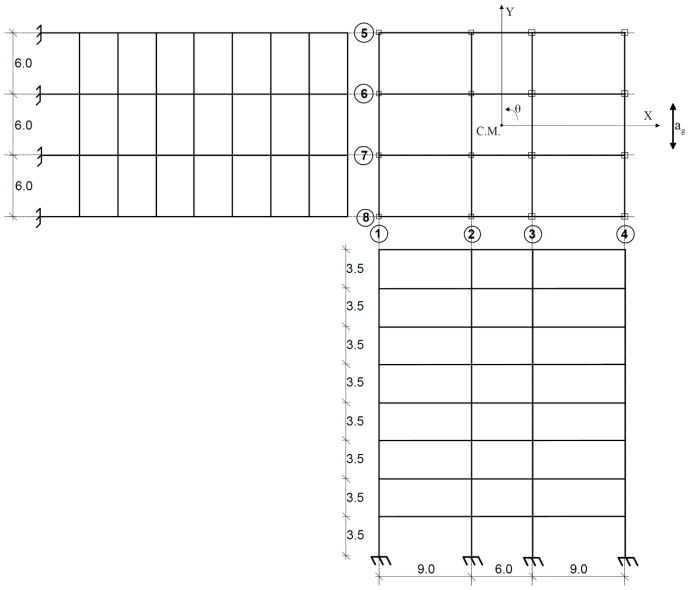

Figure 4: eight-story asymmetric structure.

Step 1: The mass, inherent damping and stiffness matrices of the frame in the dynamic DOFs shown in Fig. 1 were constructed.

Step 2: The natural frequencies, of the structure were determined. The first 10 frequencies are presented in Table 1.

Mode no.	Angular frequency (rad/sec)	Mode direction	Mode no.	Angular frequency (rad/sec)	Mode direction
1	5.135	x	6	22.407	y,θ
2	5.463	y,θ	7	29.649	x
3	7.087	y,θ	8	29.876	y,θ
4	16.240	x	9	40.918	y,θ
5	16.938	y,θ	10	44.770	y,θ

Table 1: Frequencies of the structure.

Step 3: The RMS accelerations of the undamped building at the peripheral frames in the "y" direction are presented in Fig. 5. Those were obtained using the Kanai-Tajimi PSD with parameters: $\omega_g = 13 rad/\sec$, $\xi_g = 0.98$ and $S_0 = 1$. Those parameters were determined by fitting the parameters ω_g and ξ_g to a spectrum of mean FFT values of the SE 10 in 50 ground-motion ensemble, scaled to S_0=1.0 (see Fig. 6). The actual value of S_0 has no effect since the allowable RMS acceleration is determined by the percentage of reduction desired. The allowable RMS acceleration for all peripheral accelerations was earlier adopted as 60% of the maximum peripheral RMS acceleration of the bare frame, giving: $a_{\text{all}}^{\text{RMS}} = 15.95$. It is assumed, as a first guess, that a similar reduction would be achieved in the envelope peak acceleration in time domain.

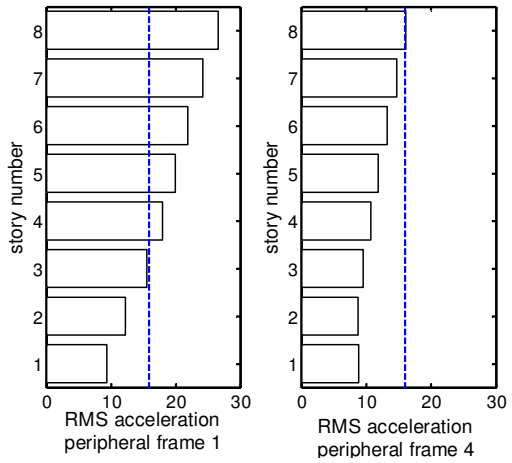

Figure 5: Peripheral RMS accelerations of bare structure (continuous) and allowable values (dashed).

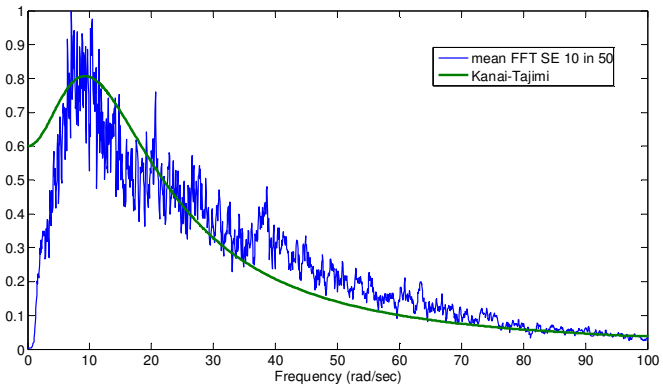

Figure 6: chosen input power-spectral-density.

Step 4: 160 TMDs were added, as a first guess, with initial properties as given in Table 2. Those are comprised of 10 dampers each tuned to a different mode frequency (of modes related to "y" and "θ") at each of the 16 peripheral locations of frames 1 and 4.

No. TMD	mode to dampen	Initial mass (ton)	Initial natural frequency (rad/sec)	Initial damping ratio
1-16	2	2.592	5.37	0.0788
17-32	3	2.592	6.89	0.1004
33-48	5	2.592	16.64	0.0795
49-64	6	2.592	21.78	0.0998
65-80	8	2.592	29.34	0.0805
81-96	9	2.592	39.79	0.0989
97-112	11	2.592	43.94	0.0816
113-128	12	2.592	60.28	0.0822
129-144	13	2.592	62.30	0.0983
145-160	15	2.592	77.55	0.0826

Table 2: Initial properties of TMDs.

Step 5: The mass, stiffness and damping matrices were updated using Eqs. (20) - (25).

Step 6: With the newly-updated matrices and the same PSD input, new peripheral RMS accelerations, shown in Fig. 7 (for frames 1 and 4), were evaluated using Eq. (8) – (12). Peripheral accelerations smaller than the allowable, were attained for all floors of frames 5 and 8 (see Fig, 4 for frame numbering).

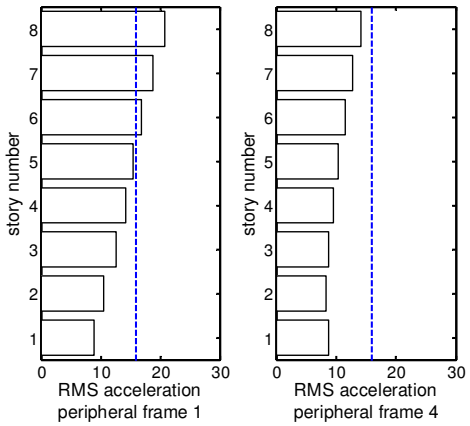

Figure 7: Peripheral RMS accelerations of structure with initial TMDs (continuous) and allowable values (dashed).

Step 7: The problem has not converged, and thus the TMDs' properties were altered, using the recurrence relations of Eqs. (28) and (29), while using P=2 as the convergence parameter, giving updated total masses at each DOF. For example, the newly updated mass of all TMDs at floor 1 of peripheral frame 1 is: $m_{TMD,1}^{(1)} = 2.592 \cdot \left(\frac{9.41}{15.92} \right)^2 = 0.906$ for a RMS total acceleration of 9.41 at that location (frame 1, 1st floor) after adding initial TMDs (Fig. 7). The total mass of each peripheral coordinate was then distributed between the 10 dampers at the same location using Eq. (29).

Step 8: Iterative analysis/redesign as described in Eqs. (28) and (29) while altering the mass of the damper is carried out until convergence to allowable levels. Upon convergence the dampers' total mass at each location are shown in Table 3.

TMDs with non-zero properties were located at frames number 1 and 4 at, both at the 8th floor, which is the top floor of each peripheral frame. The final properties of each added TMD are shown in Table 4. For frame number 1, the TMDs are set to dampen mode 2, while for frame number 4, the TMDs are set to dampen modes 2 and 3.

floor	Total mass frame 1	Total mass frame 4
1-7	0	0
8	112.69	6.25

Table 3: Total mass of TMDs upon convergence

frame	floor	mode to dampen	Final mass (ton)	Final stiffness (kN/m)	Final damping ratio
1	8	2	112.69	2472.15	0.1983
4	8	2	5.69	124.89	0.1983
4	8	3	0.55	27.72	0.0209

Table 4: Final properties of added TMDs

Finally, an analysis of the retrofitted structure yields the peripheral RMS accelerations shown in Fig. 8.

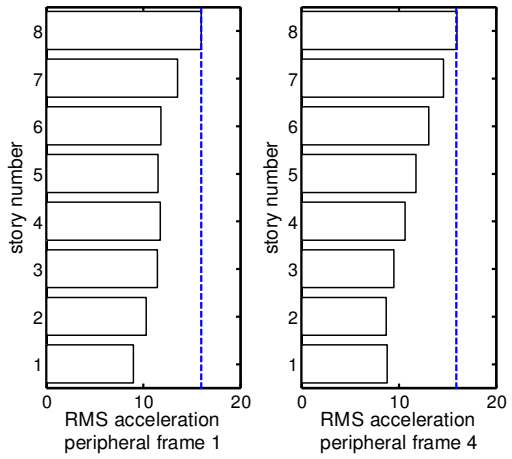

Figure 8: Peripheral RMS accelerations of structure with final TMDs (continuous) and allowable values (dashed).

All 4 assigned TMDs add up to 4.59% of the original structure's mass. As can be seen, only floors who had reached the maximum allowable RMS total acceleration (Fig. 8) were assigned with added absorbers (Table 4), making the solution obtained a FSD.

Fig. 9 presents the convergence of the design variables (masses) and the performance measure (acceleration). As can be seen in Fig. 9, although the initial guess was very far from optimum, convergence is practically reached within less than 40 iterations.

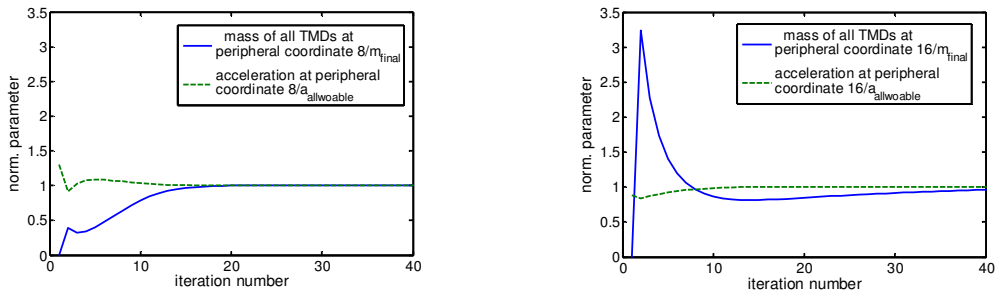

(a) (b)

Figure 9: Convergence of sum of masses and RMS acceleration at (a) 8th floor of peripheral frame number 1 and (b) 8th floor of peripheral frame number 4.

Step 9: The retrofitted structure was examined using time-history analysis under the SE 10 in 50 ensemble of real recorded earthquakes, scaled by a factor of 0.8, to check the validity of the solution obtained. The results of the envelope peak peripheral total accelerations and inter-story drifts of frames 1 and 4 obtained using time-history analysis are shown in Fig. 10. Smaller accelerations were attained in frames 5 and 8.

The results reveal that for this ensemble, the envelope maximum total acceleration of all locations of the bare structure was at the 8th floor of frame number 1, equaling 1.34g, while the envelope maximum total acceleration of all locations of the damped structure was 1.11g

(8^{th} floor of frame 4). This represents a 17% reduction in acceleration response, not so close to the desired reduction of 40% in maximum response.

Although reducing the drifts was not part of the design process, it can be seen that these too were appreciably reduced. The maximum peripheral drift of all locations was reduced from 1.95% in the bare structure to 1.30% in the damped structure.

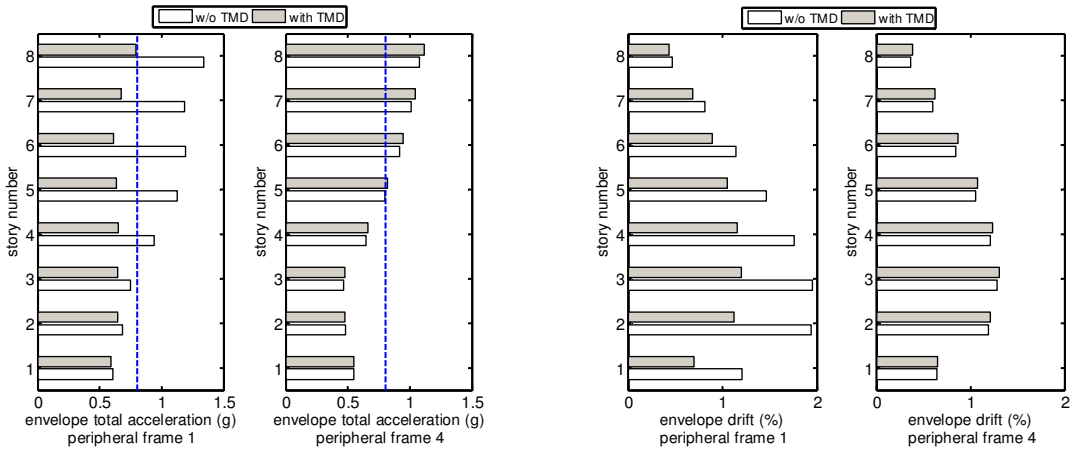

(a) (b)

Figure 10: Peripheral envelope (a) accelerations and allowable values (dashed) and (b) drifts of the bare and damped structure under the SE 10 in 50 ground motion ensemble.

Step 10: For a more accurate design, the allowable RMS total acceleration of each story is modified to better reflect the allowable peak acceleration, using Eq. (30).

In this case, a 40% reduction in envelope peak acceleration is desired, thus $a_{\text{all}}^{\text{t}} = 0.6 \cdot \max_{l}\left(\max_{eq}\left(\max_{t}\left(\left(\ddot{\mathbf{x}}_{\text{p}}^{\text{t}}(t)_{bare-frame}\right)_{l}\right)\right)\right) = 0.6 \cdot 1.34 = 0.804g$). For example, for location 8 (frame 1, 8^{th} floor): $a_{\text{all},8}^{\text{RMS}} = 0.804 \cdot \frac{15.952}{0.795} = 16.15$. Using this modification, the analysis/redesign process (steps 5-9) is repeated until convergence is once again reached. After convergence, the total mass was increased to 8.36% of the structure's mass. The modified retrofitted structure was again examined using time-history analysis under the SE 10 in 50 ensemble scaled by a factor of 0.8. The reduction between maximal envelope acceleration of all floors of the bare and damped structure was increased to 34.8%. The results can be modified yet again using step 10. After the third modification, the added mass of all TMDs increased to 8.87% (see Table 5), while the envelope peak total acceleration equaled 0.82g, representing a 39.0% reduction in response, which is very close to the desired reduction of 40%. The results of the envelope peak peripheral total accelerations and inter-story drifts of frames 1 and 4 obtained using time-history analysis are shown in Fig. 11.

frame	floor	mode to dampen	Final mass (ton)	Final stiffness (kN/m)	Final damping ratio
1	8	2	114.18	2397.4	0.2062
4	8	2	115.81	2431.7	0.2062

Table 5: Final properties of added TMDs after 3^{rd} modification

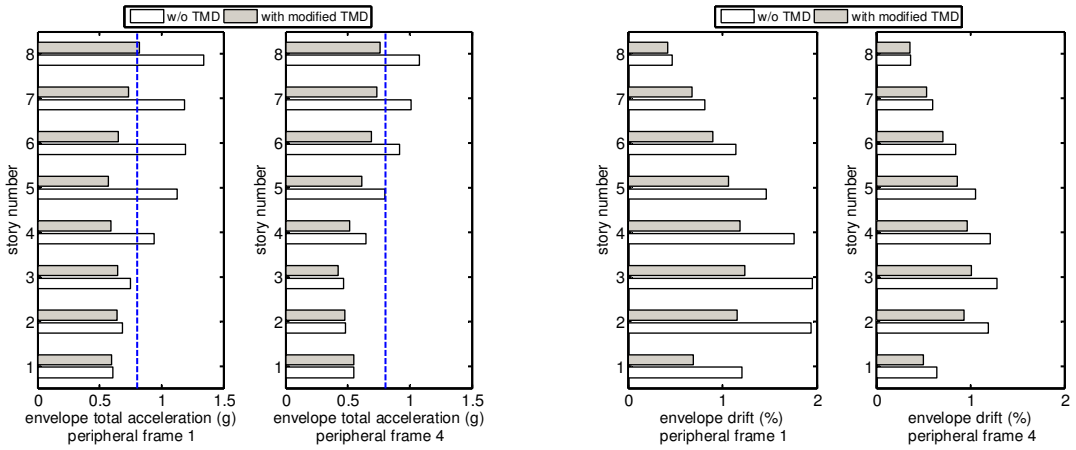

(a) (b)

Figure 11: Peripheral envelope (a) accelerations and allowable values (dashed) and (b) drifts of the bare and 3rd-time modified damped structure under the SE 10 in 50 ground motion ensemble.

6 CONCLUSIONS

An analysis/redesign frequency-domain-based methodology for optimally allocating and sizing MTMDs in 3D irregular structures was presented. The proposed methodology considers the possible dampening of all modes of the structure, at all peripheral frames, thus eliminating the decision of what modes to dampen and where the TMDs should be allocated. As shown, using MTMDs tuned to various frequencies can efficiently reduce total accelerations within the structure and bring them to a desired level, allowing for performance based design. The advantages of this methodology are its simplicity of use and relying solely on analysis tools to solve the allocation and sizing problem, with no assumptions or pre-selection of any design variable. These advantages make the proposed methodology very attractive and efficient for practical use.

The methodology is based on the following conjecture: *At the optimum, TMDs are assigned to peripheral locations for which the RMS total acceleration has reached the allowable value under the considered input acceleration PSD. In addition, at each location to which TMDs are added, TMDs of a given frequency are assigned only to frequencies for which the output spectral density is maximal.* And the designs are attained using a very simple analysis/redesign based methodology suggested.

As previously mentioned, detuning of the TMDs may cause major deterioration to the passive control system. Depending on the level of detuning expected, a TMD located at location l tuned to dampen mode f can be split into several smaller TMDs, each with a slightly different frequency within a bandwidth close to the natural frequency f of the main system. Thus reduction of the detuning effect and design robustness could be achieved. This could be done a-priori and taken into account in the design methodology. In cases where the damped structure is not brought to behave linearly, and damage to the structural system is apparent, the natural frequencies of the structure may change considerably. In those cases, a design according to the proposed scheme, combined with the use of semi-active TMDs (for example, [15, 16, 17]) which allow the simple change of the TMD's tuning, while still keeping the control system's low-cost, could be beneficial.

REFERENCES

[1] T.T. Soong, G.F. Dargush, *Passive Energy Dissipation Systems in Structural Engineering*. John Wiley & Sons Ltd., Chichester, England, 1997.

[2] C. Christopoulos, A. Filiatrault, *Principles of Supplemental Damping and Seismic Isolation*. Milan, Italy ,IUSS Press, 2006.

[3] J.P. Den-Hartog, *Mechanical Vibrations 2nd edition*. McGraw-Hill Book Company, Inc, 1940.

[4] G.B. Warburton, Optimum Absorber Parameters for Various Combinations of Response and Excitation Parameters. *Earthquake Engineering and Structural Dynamics*, **10**, 381-401, 1982.

[5] G.W. Housner, L.A. Bergman, T.K. Caughey, A.G. Chassiakos, R.O. Claus, S.F. Masri, R.E. Skelton, T.T. Soong, B.F. Spencer, J.T.P. Yao, Structural Control: Past, Present and Future. *Journal of Engineering Mechanics*, **123:9**, 897-971, 1997.

[6] S.G. Kelly, *Fundamentals of Mechanical Vibrations 2nd edition*. McGraw-Hill, Boston, 2000.

[7] R.J. McNamara, Tuned Mass Dampers for Buildings. *ASCE Journal of Structural Division*, **103**, 1785-1798, 1977.

[8] R.W. Luft, Optimum Tuned Mass Dampers for Buildings. *ASCE Journal of Structural Division*, **105**, 2766-2772, 1979.

[9] K.B. Wiesner, Tuned Mass Dampers to Reduce Building Wind Motion. *ASCE Convention and Exposition*, Boston, Mass, 1-21, 1979.

[10] Y.P. Gupta, A.R. Chandrasekaran, Absorber System for Earthquake Excitation. *Proceedings of the 4th world Conference on Earthquake Engineering*, Santiago, Chile, **II**, 139-148, 1969.

[11] A.M. Kaynia, D. Veneziano, J.M. Biggs, Seismic Effectiveness of Tuned Mass Dampers. *ASCE Journal of Structural Division*, **107**, 1465-1484, 1981.

[12] J.K. Sladek, R.E. Klingner, Effect of Tuned-Mass Dampers on Seismic Response. *ASCE Journal of Structural Division*, **109**, 2004-2009, 1983.

[13] A.H. Chowdhury, M.D. Iwuchukwu, J.J. Garske, The Past and Future of Seismic Effectiveness of Tuned Mass Dampers. *Proceedings of the Second International Symposium on Structural Control*, Ontario, Canada, 105-127, 1985.

[14] S.K. Rasouli, M. Yahyai, Control of Response of Structures with Passive and Active Tuned Mass Dampers. *The Structural Design of Tall Buildings*, **11**, 1-14, 2002.

[15] S. Nagarajaiah, E. Sonmez, Structures with Semiactive Variable Stiffness Single/Multiple Tuned Mass Dampers. *Journal of Structural Engineering*, **133:1**, 67-77, 2007.

[16] S. Nagarajaiah, Adaptive Passive, Semiactive, Smart Tuned Mass Dampers: Identification and Control using Empirical Mode Decomposition, Hilbert Transform, and Short-Term Fourier Transform. *Structural Control and Health Monitoring*, **16**, 800-841, 2009.

[17] A.J. Roffel, R. Lourenco, S. Narasimhan, Experimental Studies on an Adaptive Tuned Mass Dampers with Real-time Tuning Capability. *ASCE 19th Analysis & Computation Specialty Conference*, 314-324, 2010.

[18] M. Abdel-Rohman, Optimal Design of Active TMD for Buildings control. *Building and Environment*, **19:3**, 191-195, 1984.

[19] K. Xu, T. Igusa, Dynamic Characteristics of Multiple Substructures with Closely Spaced Frequencies. *Earthquake Engineering and Structural Dynamics*, **21**, 1059-1070, 1992.

[20] A.J. Clark, Multiple Passive Tuned Mass Dampers for Reducing Earthquake Induced Building Motion. *Proceedings of the 9th World Conference on Earthquake Engineering*, Tokyo-Kyoto, Japan, **V**, 779-784, 1988.

[21] K.S. Moon, Vertically Distributed Multiple Tuned Mass Dampers in Tall Buildings: Performance Analysis and Preliminary Design. *The Structural Design of Tall and Special Buildings*, **19**, 347-366, 2010.

[22] K.S. Moon, Integrated Damping Systems for Tall Buildings: Vertically Distributed TMDs. *2010 ASCE Structures Congress*, 3122-3131, 2010.

[23] P.H. Wirsching, G.W. Campbell, Minimal Structural Response under Random Excitations using Vibration Absorber. *Earthquake Engineering and Structural Dynamics*, **2**, 303-312, 1974.

[24] F. Sadek, B. Mohraz, A.W. Taylor, R.M. Chung, R.M., A Method of Estimating the Parameters of Tuned Mass Dampers for Seismic Applications. *Earthquake Engineering and Structural Dynamics*, **26**, 617-635, 1997.

[25] C.L. Lee, Y.T. Chen, L.L. Chung, Y.P. Wang, Optimal Design Theories and Applications of Tuned Mass Dampers. *Engineering Structures*, **28**, 43-53, 2006.

[26] M.N.S Hadi, Y. Arfiadi, Optimum Design of Absorber for MDOF Structures. *Journal of Structural Engineering*, **124: 11**, 1272-1280, 1998.

[27] B.F. Spencer, J. Suhardjo, M.K. Sain, Frequency Domain Optimal Control Strategies for Aseismic Protection. *Journal of Engineering Mechanics*, **120:1**, 135-158, 1994.

[28] T.T. Soong, State of the Art Review – Active Structural Control in Civil Engineering. *Engineering Structures*, **10**, 74-84, 1988.

[29] T.T. Soong, *Active Structural Control: Theory and Practice*. Harlow, England: Longman Scientific & Technical, 1990.

[30] Z. Prucz, T.T. Soong, A.M. Reinhorn, An Analysis of Pulse Control for Simple Mechanical Systems. *ASME Journal of Dynamic* Systems, Measurement and Control, **107**, 123-131, 1985.

[31] C.H. Chuang, D.N. Wu, Optimal Bounded-State Control with Applications to Building Structure. *Optimal Control Applications and Methods*, **17**, 209-230, 1996.

[32] C.H. Chuang, D.N. Wu, Q. Wang, LQR for State-Bounded Structural Control. *ASME Transactions Journal of Dynamic Systems, Measurement and Control*, **118**, 113-119, 1996.

[33] A. Del Grosso, A. Zucchini, Bounded-State Active Control of Structures: a Set-Theoretic Approach. *Smart Materials and Structures*, **4**, A15-A24, 1995.

[34] G. Chen, J. Wu, Optimal Placement of Multiple Tune Mass Dampers for Seismic Structures. *Journal of Structural Engineering*, **127:9**, 1054-1062, 2001.

[35] X. Luo, R. Ma, G. Li, D. Zhao, Parameter Optimization of Multi-Mode Vibration Control System. *International Conference of Measuring Technology and Mechatronics Automation*, IEEE Computer Society, 685-688, 2009.

[36] C.C. Lin, J.F. Wang, C.H. Lien, H.W. Chiang, C.S. Lin, Optimum Design and Experimental Study of Multiple Tuned Mass Dampers with Limited Stroke. *Earthquake Engineering and Structural Dynamics*, **39**, 1631-1651, 2010.

[37] T.S. Fu, E.A. Johnson, Distributed Mass Damper System for Integrating Structural and Environmental Control in Buildings. *Journal of Engineering Mechanics*, in press (doi:10.1061/(ASCE)EM.1943-7889.0000211), 2011 .

[38] F.H. Cilley, The Exact Design of Statically Indeterminate Frameworks, An Exposition of its Possibility but Futility. *ASCE Transactions,* **43**, 353-407, 1990.

[39] R. Levy, On the Optimal Design of Trusses under One Loading Condition. *Quarterly of Applied Mathematics*, **43:2**, 129-134, 1985.

[40] R. Levy, O. Lavan, Fully Stressed Design of Passive Controllers in Framed Structures for Seismic Loadings. *Journal of Structural and Multidisciplinary Optimization*, **32**, 485-498, 2006.

[41] K. Kanai, Semi-Empirical Formula for the Seismic Characteristics of the Ground. *Bulletin of Earthquake Research Institute*, University of Tokyo, **35**, 309-325, 1957.

[42] S. Nagarajaiah, S. Narasimhan, Smart Base-Isolated Benchmark Building. Part II: Phase I Sample Controllers for Linear Isolation Systems. *Structural Control and Health Monitoring*, **12**, 589-604, 2006.

[43] A.K. Agrawal, Z. Xu, W.L. He, Ground Motion Pulse-Based Active Control of a Linear Base-Isolated Benchmark Building. *Structural Control and Health Monitoring*, **13**, 792-808, 2006.

[44] H. Kwakernaak, R. Sivan, *Modern Signals and Systems*. Englewood Cliffs, NJ, Prentice Hall Inc., 1991.

[45] D.E. Newland, *An Introduction to Random Vibrations, Spectral & Wavelet Analysis.* Prentice Hall, Harlow, England, 1993.

[46] W.K. Tso, S. Yao, Seismic Load Distribution in Buildings with Eccentric Setback. *Canadian Journal of Civil Engineering*, **21**, 50-62, 1994.